

# Histones from Dying Renal Cells Aggravate Kidney Injury via TLR2 and TLR4

Ramanjaneyulu Allam,<sup>\*†</sup> Christina Rebecca Scherbaum,<sup>\*</sup> Murthy Narayana Darisipudi,<sup>\*</sup> Shrikant R. Mula,<sup>\*</sup> Holger Hägele,<sup>\*</sup> Julia Lichtnekert,<sup>\*</sup> Jan Henrik Hagemann,<sup>\*</sup> Khader Valli Rupanagudi,<sup>\*</sup> Mi Ryu,<sup>\*</sup> Claudia Schwarzenberger,<sup>‡</sup> Bernd Hohenstein,<sup>‡</sup> Christian Hugo,<sup>‡</sup> Bernd Uhl,<sup>§</sup> Christoph A. Reichel,<sup>§</sup> Fritz Krombach,<sup>§</sup> Marc Monestier,<sup>||</sup> Helen Liapis,<sup>||</sup> Kristin Moreth,<sup>\*\*</sup> Liliana Schaefer,<sup>\*\*</sup> and Hans-Joachim Anders<sup>\*</sup>

<sup>\*</sup>Medizinische Klinik und Poliklinik IV, Klinikum der Universität München, Munich, Germany; <sup>†</sup>Department of Biochemistry, University of Lausanne, Epalinges, Switzerland; <sup>‡</sup>Division of Nephrology, University of Dresden, Dresden, Germany; <sup>§</sup>Walter Brendel Centre of Experimental Medicine, University of Munich, Munich, Germany; <sup>||</sup>Temple Autoimmunity Center, Department of Microbiology and Immunology, Temple University School of Medicine, Philadelphia, Pennsylvania; <sup>||</sup>Department of Pathology and Immunology, Washington University School of Medicine, St. Louis, Missouri; and <sup>\*\*</sup>Institut für Allgemeine Pharmakologie und Toxikologie, Klinikum der Goethe-Universität, Frankfurt am Main, Germany

## ABSTRACT

In AKI, dying renal cells release intracellular molecules that stimulate immune cells to secrete proinflammatory cytokines, which trigger leukocyte recruitment and renal inflammation. Whether the release of histones, specifically, from dying cells contributes to the inflammation of AKI is unknown. In this study, we found that dying tubular epithelial cells released histones into the extracellular space, which directly interacted with Toll-like receptor (TLR)-2 (TLR2) and TLR4 to induce MyD88, NF- $\kappa$ B, and mitogen activated protein kinase signaling. Extracellular histones also had directly toxic effects on renal endothelial cells and tubular epithelial cells *in vitro*. In addition, direct injection of histones into the renal arteries of mice demonstrated that histones induce leukocyte recruitment, microvascular vascular leakage, renal inflammation, and structural features of AKI in a TLR2/TLR4-dependent manner. Antihistone IgG, which neutralizes the immunostimulatory effects of histones, suppressed intrarenal inflammation, neutrophil infiltration, and tubular cell necrosis and improved excretory renal function. In summary, the release of histones from dying cells aggravates AKI via both its direct toxicity to renal cells and its proinflammatory effects. Because the induction of proinflammatory cytokines in dendritic cells requires TLR2 and TLR4, these results support the concept that renal damage triggers an innate immune response, which contributes to the pathogenesis of AKI.

*J Am Soc Nephrol* 23: 1375–1388, 2012. doi: 10.1681/ASN.2011111077

AKI involves a significant sterile inflammatory response that contributes to the extent of tubular necrosis and renal dysfunction.<sup>1,2</sup> In this regard, postischemic AKI resembles ischemic injuries in other organs (e.g., in the heart during myocardial infarction, in the brain during ischemic stroke, or in skeletal muscles during limb ischemia).<sup>3</sup> In all these conditions, reperfusion of ischemic tissue is associated with the production of reactive oxygen species that activate tissue cells to secrete proinflammatory cytokines and chemokines. This process recruits neutrophils and activated macrophages that exaggerate

Received November 15, 2011. Accepted May 2, 2012.

R.A., C.R.S., and M.N.D. contributed equally to this work.

Published online ahead of print. Publication date available at [www.jasn.org](http://www.jasn.org).

**Correspondence:** Dr. Hans-Joachim Anders, Medizinische Klinik und Poliklinik IV, Klinikum der Universität München, Pettenkoferstr. 8a, D-80336 Munich, Germany. Email: [hjanders@med.uni-muenchen.de](mailto:hjanders@med.uni-muenchen.de)

Copyright © 2012 by the American Society of Nephrology

organ inflammation, tissue injury, and malfunction.<sup>1</sup> During the past decade it has become evident that the initiation of this sterile inflammatory response is largely based on the activation of Toll-like receptors (TLRs). TLRs are germline encoded pattern-recognition receptors that have important roles in innate immunity against all sorts of pathogens by recognizing various pathogen-associated molecular patterns.

In a major breakthrough in the understanding of noninfectious types of inflammation, TLRs were found to also recognize endogenous damage-associated molecular patterns (DAMPs), which have identical properties to activate innate immunity and tissue inflammation as pathogens.<sup>3</sup> This concept was first established by showing that necrotic cells trigger cytokine production and neutrophil recruitment *via* TLRs and its dominant signaling adaptor MyD88.<sup>4,5</sup> Subsequent work has identified several endogenous intracellular molecules that have the potential to activate TLR signaling and cytokine secretion, such as high-mobility group protein (HMG) B1 (TLR2, TLR4, and the receptor for advanced glycation end products [RAGE]), as well as hypomethylated CpG-DNA (TLR9).<sup>4</sup> In support of this concept, mice deficient for TLR2, TLR4, or MyD88 or mice treated with HMGB1-blocking antibodies are protected from posts ischemic intrarenal inflammation, which largely prevents tubular cell necrosis and acute renal failure.<sup>6–9</sup> The same evidence is available for ischemia-reperfusion injuries in other organs, such as the liver,<sup>10</sup> the heart,<sup>11,12</sup> and the brain.<sup>13</sup> Our work reported here is based on the assumption that additional intracellular molecules that can act as DAMPs and sense renal tissue damage to the immune system remain to be discovered.<sup>14</sup>

Histones are a group of nuclear proteins that form hetero-octamers to wind up the double-stranded DNA to form chromatin as well as chromosomes. Histones are released from dying neutrophils during bacterial infections for host defense, the so-called neutrophil extracellular traps (NETs).<sup>15,16</sup> The bactericidal effect of extracellular histones also damages self tissues.<sup>17</sup> For example, histone release directly contributes to fatal outcomes in murine endotoxemia by activating and killing vascular endothelial cells.<sup>18</sup> We therefore speculated that chromatin release from dying renal cells would shuttle histones in the extracellular space, where they act as DAMPs by activating one or more pattern recognition receptors. In addition, we speculated that this process would contribute to sterile inflammation during posts ischemic kidney injury as well as to septic AKI.

Because of the essential role of histones for chromatin assembly, histone-deficient mice could not be generated to test our concept experimentally. In fact, it was necessary to neutralize histones specifically in the extracellular compartment, which became possible by using the same histone-specific IgG and control IgG that have been used by others for similar *in vitro* and *in vivo* studies.<sup>18</sup> Here we report that dying tubular epithelial cells release histones into the extracellular space, thereby contributing to posts ischemic and septic kidney inflammation and injury. Furthermore, we report that extracellular histones

directly activate and potentially kill renal endothelial and tubular cells. In addition, both TLR2 and TLR4 are required to translate histone recognition into MyD88 signaling and the secretion of proinflammatory mediators.

## RESULTS

### Histones Are Released from Necrotic Tubular Epithelial Cells

Our concept of histones being an endogenous danger signal to activate renal inflammation is based on the assumption that dying renal cells release histones into extracellular compartments. In fact, immunoblotting for histones revealed a strong positivity for histones in cell culture supernatants of hydrogen peroxide-treated tubular epithelial cells similar to cells killed by repetitive freeze-thawing after 24 hours (Figure 1A).

### Extracellular Histones Kill Renal Endothelial Cells and Tubular Epithelial Cells

Extracellular histones have been reported to promote fatal sepsis by directly damaging the pulmonary microvasculature.<sup>18</sup> To test a putative toxic role of histones on renal cells, we incubated murine renal endothelial cells or tubular epithelial cells with a total histone preparation. Endothelial and tubular cell viability was reduced in a dose-dependent manner within 24 hours, whereas agonists for TLR2, -4, and -9 had no effect (Figure 1B). Next we analyzed the supernatants of the endothelial cell experiments by flow cytometry for nonadherent annexin V/propidium iodine-double-positive (apoptotic) cells and annexin V-negative/propidium iodine-positive (necrotic) cells. Histone exposure increased both types of cells in a dose-dependent manner within 24 hours (Figure 1D). Thus, extracellular histones negatively affect the viability of renal endothelial and tubular cells.

### Extracellular Histones Increase Leukocyte Adhesion and Microvascular Permeability

We used *in vivo* microscopy on mouse cremaster muscles to study whether histone exposure induces leukocyte recruitment and enhances microvascular permeability. After 6 hours of local histone application, there was a significant elevation in leukocyte intravascular adherence and transendothelial migration compared with controls (Figure 2, A–D). Immunostaining of cremaster muscles identified  $90.0\% \pm 2.6\%$  of transmigrated CD45<sup>+</sup> cells (total leukocytes) as Ly-6G<sup>+</sup> cells (neutrophils) and the rest as F4/80<sup>+</sup> (monocytes/macrophages). In addition, histone exposure significantly increased leakage of FITC dextran into the interstitial compartment (Figure 2, E and F). When histones were preincubated with activated protein C, an enzyme that digests histones (Figure S1A), the histone-related effects were abrogated (Figure 2, B, C, and E). Leukocyte recruitment and microvascular permeability significantly increase when the microvasculature is exposed to extracellular histones.

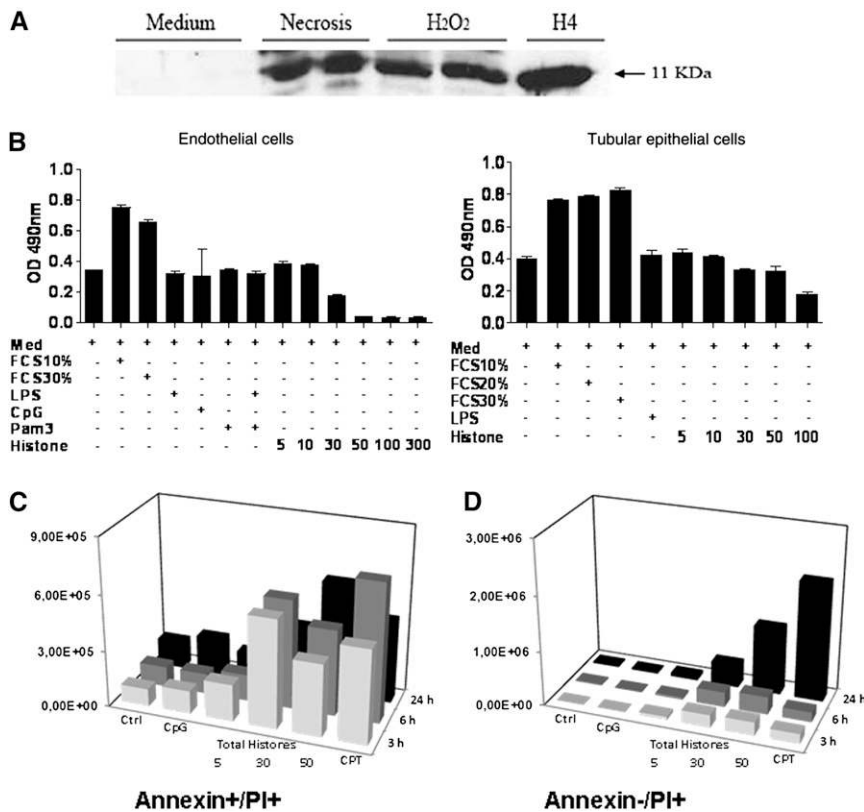


**Figure 1.** Dying renal cells release histones into extracellular compartments. (A) Necrosis was induced in primary tubular epithelial cells as described in the Concise Methods section. Histone H4 was detected in necrotic supernatants by using anti-H4 antibody. Recombinant histone H4 was loaded as a positive control. (B) Renal endothelial cell proliferation was determined in a period of 24 hours by bioluminescence assay, as described in the Concise Methods. Data represent mean OD  $\pm$  SEM of three experiments measured at a wavelength of 492 nm. (C and D) Renal endothelial cells were stimulated with CpG, 6  $\mu$ g/ml; camptothecin (CPT), 10  $\mu$ M; or histones. Doses are given in  $\mu$ g/ml. Results show flow cytometry from floating cells in culture supernatants. Data represent the mean of total positive cell numbers of positive cells of three independent experiments. PI, propidium iodide.

### Histone Injection into the Renal Artery Induces Renal Cell Necrosis

Next we sought to study the effects of extracellular histones on the kidney. Because intravenous histone injection kills mice immediately *via* severe alterations of the pulmonary microvasculature,<sup>18</sup> we injected histones directly into the left renal artery of anesthetized mice (Figure 3A). Unilateral histone injection led to widespread necrosis of the renal cortex and outer medulla and massive neutrophil infiltrates after 24 hours, whereas the contralateral kidney remained unaffected (Figure 3B). Electron microscopy displayed that LPS injection alone had already led to dilation of peritubular capillaries and interstitial edema but that histone injection aggravated vascular dilation and induced condensation of microvascular endothelial cell chromatin, implying apoptosis (Figure 3C). Histone-induced renal cell necrosis was associated with an increase in renal mRNA expression of multiple proinflammatory mediators, such as IL-6,

TNF- $\alpha$ , and inducible nitric oxide synthase (Figure 3D). When the histones were pre-digested with activated protein C (Supplemental Figure 1A) or when the identical experiment was conducted in *Tlr2/4*-deficient mice, renal necrosis, neutrophil recruitment, and cytokine expression were significantly reduced compared with results seen when histone was injected into wild-type mice (Figure 3, B and C and Supplemental Figure 1B). This histone effect was absent without a systemic intravenous injection of a nontoxic dose of endotoxin (1.0 mg/kg body weight) 12 hours before histone injection (Supplemental Figure 2), which was necessary to induce renal TLR2 and TLR4 expression (Figure 3E). Previous studies had already excluded any effect due to the injection procedure itself.<sup>19</sup> Thus, extracellular histones massively aggravate renal inflammation and renal cell necrosis.

### Histone Neutralization Reduces Endotoxin-Induced AKI

Do extracellular histones also contribute to septic AKI? To address this issue, we used a neutralizing antibody to histones that was previously used to establish the functional contribution of extracellular histones in lethal endotoxemia in mice.<sup>18</sup> Mice were injected with 20 mg/kg antihistone IgG or with 20 mg/kg control IgG 2 hours before the intraperitoneal injection of LPS (10 mg/kg). Antihistone IgG administration significantly reduced serum creatinine levels at 12 hours after LPS injection (Figure 4). This reduction was associated with a significant decrease in septic tubular injury, as assessed by semiquantitative morphometry (Figure 4). In addition, renal neutrophil counts were significantly reduced with histone blockade (Figure 4). We conclude that extracellular histones contribute to AKI in murine endotoxemia.

### Histone H4 Neutralization Reduces Renal Ischemia-Reperfusion Injury

Do extracellular histones also contribute to postischemic AKI? Injection of antihistone IgG immediately after bilateral renal-artery clamping prevented postischemic tubular damage 24 hours after surgery compared with treatment with control IgG (Figure 5). This finding was quantified by semiquantitative scoring using a composite score of brush border loss, tubular cell flattening, tubular cell necrosis, and granular cast formation. Distal tubules were protected by antihistone IgG, as determined by staining for Tamm-Horsfall protein, whereas proximal tubular cells, identified with tetragonolobus lectin

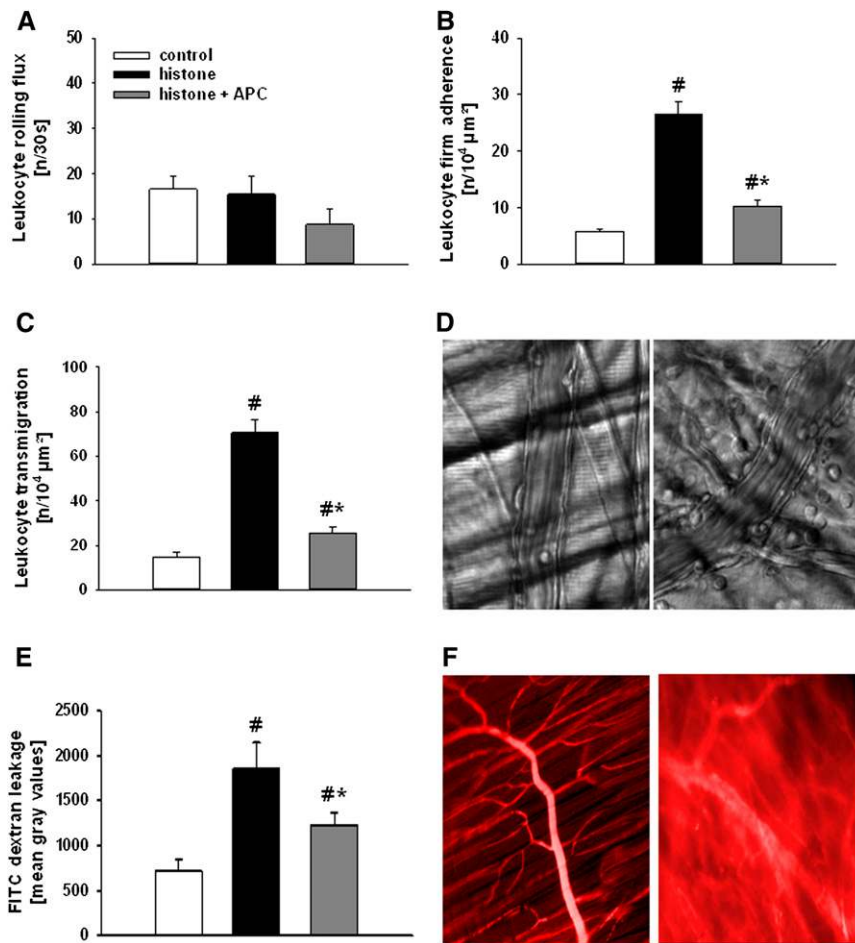


**Figure 2.** *In vivo* microscopy of cremaster muscles. *In vivo* microscopy was performed on cremaster muscle postcapillary venules as described in the Concise Methods section. Six mice in each group were treated with intrascrotal injections of vehicle or total histones as indicated. Leukocyte rolling (A), firm adhesion (B), and transendothelial migration (C) were determined 6 hours after injection. Histone+APC means that histone had been pre-incubated with activated protein C (APC) before injection. Data are means  $\pm$  SEM. # $P$ <0.05 versus control, \* $P$ <0.05 versus histones. (D) Representative images illustrate the increase in leukocyte adhesion and transendothelial migration after histone challenge (right) versus control (left). (E) Microvascular FITC-dextran leakage was determined 6 hours after injection. Data are means  $\pm$  SEM. # $P$ <0.05 versus control, \* $P$ <0.05 versus histones. (F) Representative images illustrate the increase in vascular dextran permeability after histone challenge (right) versus control (left).

staining, were not significantly preserved (Figure 5). The numbers of terminal deoxynucleotidyl transferase-mediated digoxigenin-deoxyuridine nick-end labeling (TUNEL)-positive renal cells were significantly reduced in antihistone-treated mice (Figure 5), indicating less tubular cell apoptosis in the postischemic kidney. This improvement in structural damage was associated with significantly reduced blood urea nitrogen levels 24 hours after surgery ( $117 \pm 25$  versus  $58 \pm 2$ ;  $P=0.02$ ), suggesting that antihistone IgG prevented loss of renal excretory function during postischemic AKI. Extracellular chromatin has been reported to trigger tissue inflammation;<sup>18,20,21</sup>

hence, we assessed the intrarenal mRNA expression of proinflammatory cytokines in both treatment groups. Antihistone IgG significantly reduced the renal mRNA levels of the tubular injury marker KIM-1, which was associated with lower mRNA levels of the proinflammatory cytokines IL-6 and IL-12, the intercellular adhesion molecule, and the neutrophil-attracting chemokine CXCL2 (Figure 6A). This finding was consistent with the lower numbers of neutrophils that infiltrated the renal interstitium in antihistone-treated compared with control IgG-treated mice, especially in the areas around necrotic tubuli (Figure 6B). Together, neutralizing histones reduce the induction of cytokines and chemokines, neutrophil recruitment, tubular injury, and renal failure in the postischemic kidney.

### Histones Activate the Secretion of Proinflammatory Cytokines

Having shown that damaged tubular cells release histones and that histone neutralization reduces postischemic sterile inflammation and kidney damage, we speculated that extracellular histones directly induce the expression of proinflammatory cytokines. In fact, a total histone preparation induced the secretion of TNF and IL-6 in bone marrow-derived dendritic cells (BMDCs) (Figure 7A). Histones are protein complexes formed by <sup>1</sup>H, H2A, H2B, H3, and H4 proteins. Hence, we tested the individual proteins to induce inflammatory cytokines in BMDCs. All histone proteins induced TNF and IL-6 production (Figure 7B). However, there were differences in terms of induction in cytokine production with each protein. To further study the signaling mechanism, we used histone H4 as prototype. H4-induced NF- $\kappa$ B and mitogen activated protein (MAP) kinase activation, as shown by I $\kappa$ B- $\alpha$  degradation and p38 phosphorylation as readout for NF- $\kappa$ B and MAP kinase activation (Figure 7C). Dose- and time-dependent studies revealed that H4-induced cytokine production was most prominent at a concentration of 10  $\mu$ g for IL-6 and TNF and appeared as early as 3 hours after H4 stimulation (Supplemental Figure 2, A and B). LPS contamination did not account for this response because preincubation with polymyxin B did not affect H4-induced cytokine induction but completely blocked LPS-induced cytokine induction (Figure 7D). The immunostimulatory effect of H4 was also unaltered by preincubation with deoxyribonuclease or ribonuclease, excluding immunostimulatory nucleic

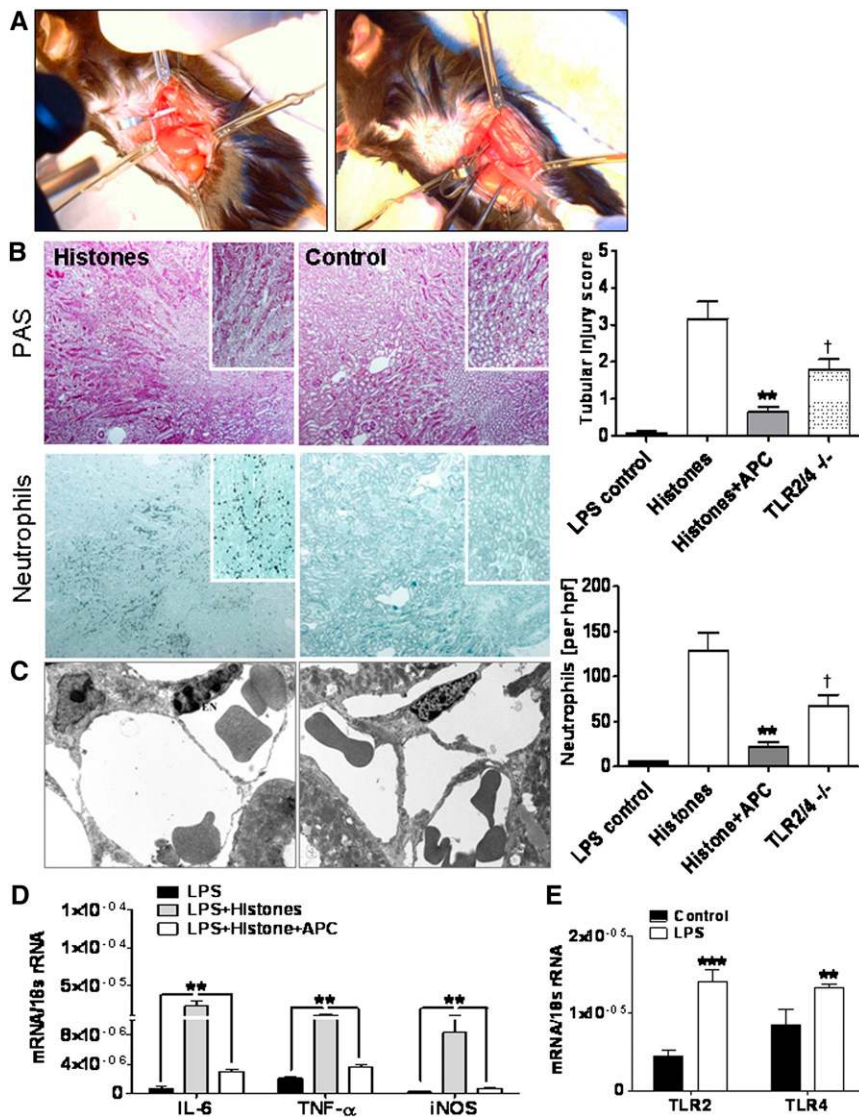


**Figure 3.** Histone injection into the renal artery. (A) Twelve hours after intraperitoneal LPS injection (1 mg/kg body weight), the abdominal aorta and the left renal artery was prepared and a microcannula was placed into the left renal artery (left) for histone injection. The puncture site was mounted with glue before closure of the wound (right). (B) Representative images of periodic acid-Schiff (PAS) stainings and for neutrophils are shown at a magnification of  $\times 50$ . The quantitative analysis of tissue injury and neutrophil numbers per high-power field are shown on the right. (C) Dilated peritubular capillaries and interstitial edema are illustrated by transmission electron microscopy. Endothelial cells with condensed nuclear chromatin seem to undergo apoptosis. Original magnification  $\times 7500$ . (D) Total kidney mRNA levels of TNF- $\alpha$ , IL-6, and inducible nitric oxide synthetase (iNOS) were determined in LPS-primed and histone-injected left kidneys. Histone preincubation (before injection) with recombinant activated protein C (APC) reduced intrarenal cytokine expression. (E) Renal mRNA levels of TLR2 and TLR4 with and without LPS priming. 18s rRNA levels were used as internal control. Data represent means  $\pm$  SEM from nine mice.  $^{\dagger}P < 0.05$ ,  $^{**}P < 0.01$ ,  $^{***}P < 0.001$  versus LPS (B and C) or saline control (D).

effect. Supporting these results, antihistone antibodies significantly reduced H4-induced TNF and IL-6 production (Figure 7F). Thus, extracellular histones are potent inducers of proinflammatory cytokine secretion.

### Both TLR2 and TLR4 Are Required for the Recognition of Histone-H4

Which pattern recognition receptors mediate these biologic effects of extracellular H4? We hypothesized that a TLR might be responsible for H4 recognition and signaling. All TLRs use MyD88 (myeloid differentiation primary response gene 88) as an adaptor molecule to induce signaling, except for TLR3, which signals through Toll/IL-1 receptor domain-containing adapter-inducing IFN $\beta$ ).<sup>22</sup> To test our hypothesis, we investigated H4 activation in *Myd88*- and *Trif*-deficient BMDCs. H4-induced TNF and IL-6 production completely abrogated in *Myd88*-deficient BMDCs (Figure 8, A and B). To test which MyD88-dependent TLR is responsible for H4 recognition, we exposed H4 to BMDCs from respective knockout mice. Deficiency of both TLR2 and TLR4 completely prevented the activation of TNF and IL-6 (Figure 5, C–E), whereas individual gene deletions of *Tlr1*, *Tlr2*, *Tlr4*, *Tlr6*, and *Cd14* did not prevent cytokine production (Figure 8, C–E). The observation that both TLR2 and TLR4 can signal for H4-induced cytokine production is similar to what has been reported for other DAMPs, such as high-mobility group protein B1<sup>9</sup> or biglycan.<sup>23</sup> HMGB1 signals through RAGE,<sup>24</sup> but we observed H4 signaling to be RAGE-independent (Figure 8F). We did not investigate TLR7 and TLR9 because endosomal acidification with chloroquine significantly abrogated CpG-induced TNF production but not H4 (Supplemental Figure 4). In addition to H4, other histone proteins also showed TLR2/TLR4 dependency (Supplemental Figures 5 and 6). Thus, extracellular histones trigger proinflammatory cytokines *via* both TLR2 and TLR4, which activates the MyD88 signaling pathway.

acid contaminations (Figure 7E). Only H4 digestion with proteinase K (Figure 7E) or activated protein C (Supplemental Figure 3) prevented cytokine induction, indicating that the peptide content of H4 was required for its immunostimulatory

### Histone-H4 Directly Interacts with TLR2 and TLR4

To check whether H4 physically interacts with TLR2 and TLR4, we performed microscale thermophoresis binding assay. The binding of NT-647 fluorescence-labeled H4 to recombinant

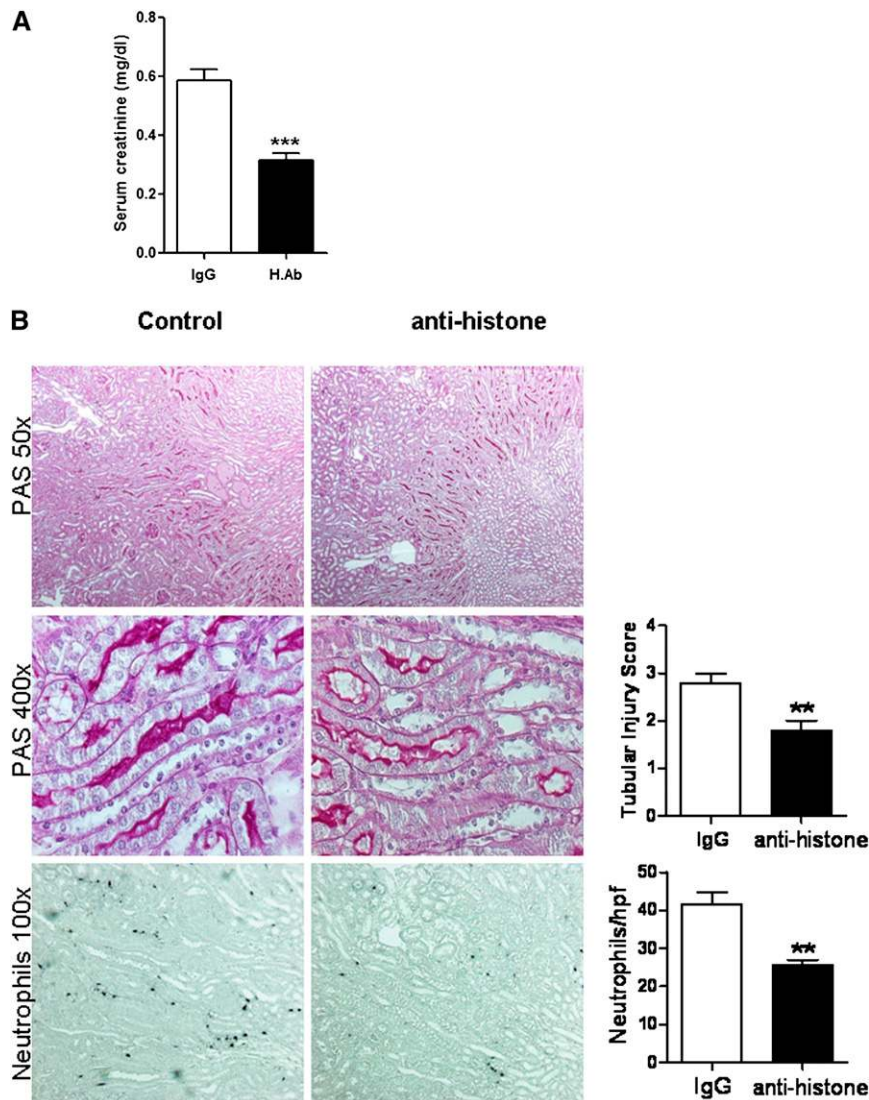


**Figure 4.** Neutralizing histone H4 protects from septic AKI. (A) Serum creatinine was determined 12 hours after intraperitoneal LPS injection. Two hours before, groups of mice had received anti-histone H4 or control IgG. Data represent means  $\pm$  SEM. \*\*\* $P < 0.001$ . (B) Renal tissue from mice of both groups was stained with periodic acid-Schiff (PAS) or for neutrophils. Representative images are shown at magnifications as indicated. Data represent means  $\pm$  SEM from six mice of each group. hpf, high-power field.

human TLR2 (Figure 9A) and TLR4/MD2 complex (Figure 9C) was analyzed by microscale thermophoresis. To determine the affinity of the binding reaction, a titration series of TLR2 (Figure 9A) and TLR4/MD2 (Figure 9C) proteins were performed, while fluorescence-labeled H4 was kept at a constant concentration of 5 nM. The change in the thermophoretic signal of H4 suggested a  $K_d$  of  $4.2 \pm 1.7$  nM ( $n=3$ ) for TLR2 (Figure 9A) and  $6.0 \pm 3.7$  nM ( $n=3$ ) for TLR4/MD2 (Figure 9C). In contrast, thermophoresis of NT-647 fluorescence-labeled albumin (5 nM, negative control) tested for its binding to TLR2 (Figure 9B) and TLR4/MD2 (Figure 9D) in the same

experimental setting, showed no dependence on TLR2 or TLR4/MD2 concentration. So these results show that H4 induces proinflammatory cytokines by directly interacting with TLR2 and TLR4. To further validate our results *in vivo*, we injected H4 protein, 20 mg/kg, intravenously into wild-type and TLR2/TLR4 double-knockout mice and measured cytokine production in the plasma after 6 hours. H4-induced IL-6 and TNF production observed in wild-type mice was abrogated with TLR2/TLR4 deficiency (Figure 9E). None of these mice displayed a renal phenotype in terms of elevated serum creatinine levels, tubular damage, or renal neutrophil infiltration (data not shown). These results show that histone H4 activates TLR2 and TLR4 to induce cytokine production in mice.

## DISCUSSION

Histones wind up DNA and regulate gene transcription inside the nucleus, but in the extracellular space histones elicit toxic and proinflammatory effects.<sup>17</sup> Hence, we had hypothesized that histone release from damaged tubular epithelial cells would promote renal inflammation in a DAMP-like fashion, implicating an interaction with distinct pattern recognition receptors. Our studies confirm this concept and identify TLR2 and TLR4 to translate histone recognition into cytokine secretion in a MyD88-dependent manner.

Acute tubular necrosis implies the release of intracellular molecules into the extracellular space. This has also been documented for nuclear particles, such as the nucleoprotein HMGB1,<sup>14,25</sup> and our *in vitro* studies demonstrate histone release from dying tubular cells, (such as occurs with exposure to oxidative stress). Elegant studies

have found that HMGB1 acts as a DAMP in sterile renal inflammation by inducing renal ischemia-reperfusion injury in mice treated with Hmgb1-blocking antibodies.<sup>9</sup> We used the same experimental strategy by applying specific histone-neutralizing antibodies that block histones in extracellular compartments *in vivo* as well as *in vitro*. Antihistone antibodies have already been used to effectively deplete extracellular histones in several *in vivo* studies, which, for example, protected from fatal endotoxemia or toxic liver injury.<sup>18,26</sup> The effects of this antibody could relate to its specific binding properties to histones compared with the effects of control IgG.

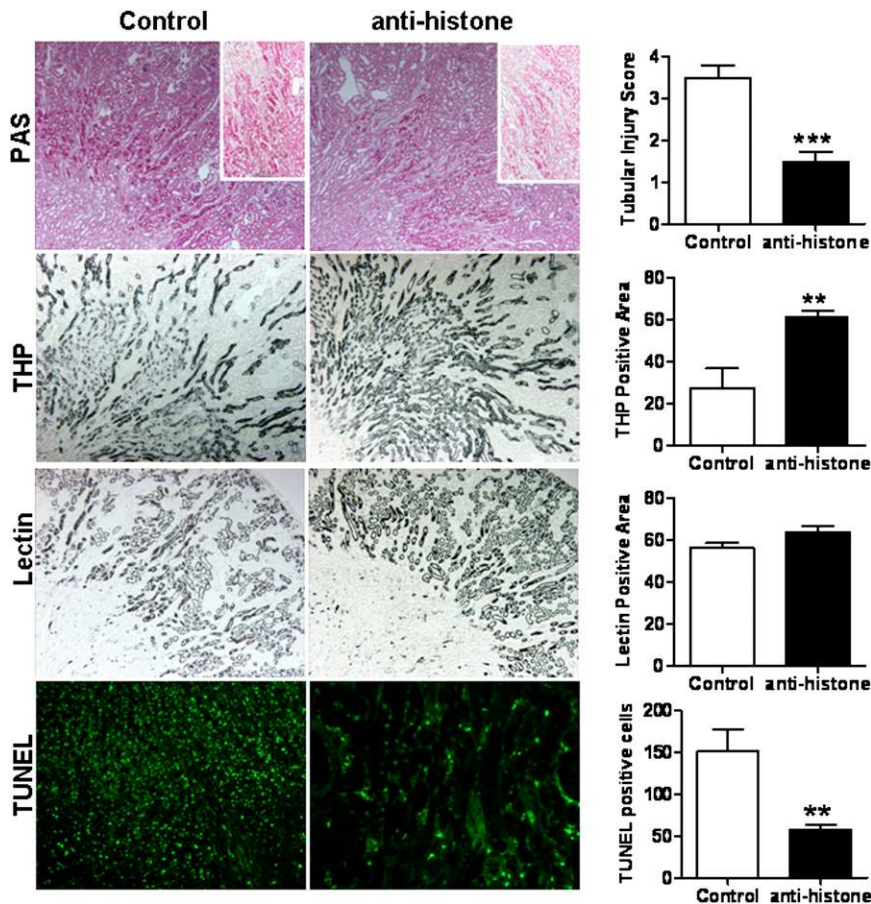


**Figure 5.** Neutralizing histone H4 improves postischemic renal pathologic findings. Renal tissue was obtained 24 hours after bilateral renal ischemia/reperfusion from anti-H4 IgG- and control IgG-treated mice and stained with periodic acid-Schiff (PAS), lectin (proximal tubular cells), Tamm-Horsfall protein (THP) (distal tubular cells), and TUNEL (apoptotic cells) as indicated. Representative images are shown at a magnification of  $\times 400$ . The quantitative analysis of tissue injury or TUNEL-positive cells is shown next to the respective staining procedure. Data represent means  $\pm$  SEM from six mice of each group. \*\* $P < 0.01$ , \*\*\* $P < 0.001$ .

As a second experimental strategy we predigested histones with activated protein C before applying them *in vivo*, before intraarterial or intrascrotal injection, which again confirmed their specific proinflammatory effects. Therefore, our *in vivo* findings document that extracellular histones contribute to septic or postischemic renal inflammation and AKI, as defined by intrarenal cytokine expression, the induction of Kim-1, neutrophil recruitment, tubular necrosis, and rise in plasma BUN or serum creatinine.

It is likely that neutrophils infiltrating the postischemic kidney also release histones because the release of the bactericidal chromatin is an effector element of neutrophil-mediated host defense (*i.e.*, NET formation).<sup>16</sup> The significance of neutrophil-derived NETs has already been documented for renal vasculitis and lupus nephritis.<sup>21,27</sup> Although the effect of anti-H4 antibody treatment could relate to systemic immunosuppressive effects in the septic AKI model, our studies using the renal

artery clamping model as well as histone injection into only one renal artery definitely prove the direct toxic and proinflammatory effect of histones on renal cells. These data are in line with the reported *in vivo* toxicity of intravenously injected histones on the pulmonary microvasculature and *in vitro* on HUVECs.<sup>18</sup> Therefore, we assume that the toxic effects of histones on tubular epithelial and glomerular endothelial cell viability also apply to peritubular endothelial cells, which were not available for *in vitro* studies. LPS priming was required for severe tissue damage, probably because LPS induced TLR2 and TLR4 inside the kidney, consistent with previous reports on endothelial and tubular epithelial cells.<sup>28–30</sup> In fact, lack of TLR2/4 partially prevented renal necrosis after histone injection. We admit that histones were injected at high concentrations in these experiments, which may not mimic the physiologic situation. However, for the *in vivo* microscopy studies a much lower histone concentration was topically applied without LPS priming; these injections still increased endothelial cell activation, leukocyte recruitment, and vascular permeability, all features of septic and postischemic AKI.<sup>1,31</sup>

Several pattern recognition receptors have been proposed to mediate the proinflammatory effects of extracellular histones.<sup>20,26</sup> Huang and colleagues' finding that TLR9 should account for histone recognition was surprising because TLR9 is a DNA receptor and TLR9 activation by such proteins as hemozoin or plasmodium histones was recently documented to relate to DNA contaminants.<sup>25,32</sup> Our *in vitro* studies clearly document that TLR2 and TLR4 are both required for histone-induced cytokine secretion. Genetic ablation of TLR2 or TLR4 alone did not abrogate IL-6 and TNF production. This observation argues against any significant LPS or bacterial lipoprotein contamination of the histone preparation because these would have been TLR2 or TLR4 dependent. Additional control experiments with deoxyribonuclease, ribonuclease, and proteinase K treatment show that the immunostimulatory effect of histone H4 refers to its protein content. In addition, anti-H4 antibodies significantly blocked H4-induced TNF and IL-6 production, which further excludes contamination of other TLR agonists. H4 induced p38 phosphorylation in 10 minutes and I $\kappa$ B- $\alpha$  degradation in 40 minutes; these results show that the activation was a primary effect of H4. TLR2/TLR4 dual-receptor binding with a *Kd* of

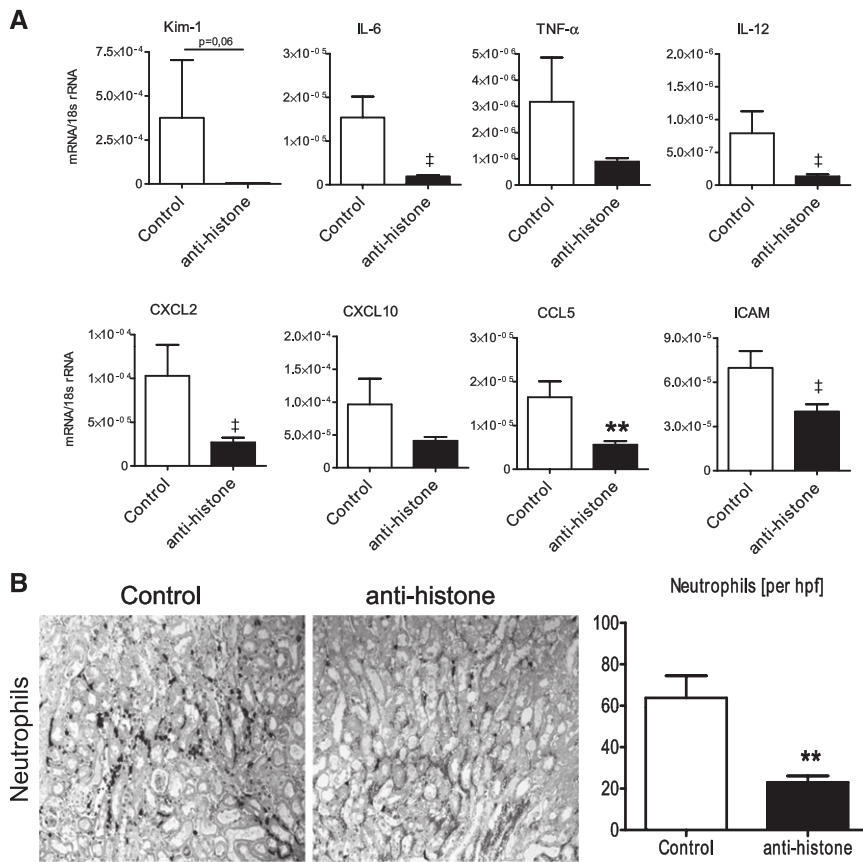


**Figure 6.** Assessment of postischemic renal inflammation. (A) Total RNA was extracted from kidneys from anti-H4 IgG- and control IgG-treated mice. KIM-1 and cytokine mRNA expression levels were determined by real-time PCR and expressed as mean of the ratio 18S rRNA ± SEM; †P<0.05 versus control. (B) Renal sections were stained for neutrophils, and representative images are shown at a magnification of ×400. The quantitative analysis of interstitial neutrophils is shown next to the respective staining procedure. Data represent means ± SEM from six mice of each group. \*\*P<0.01.

4.2±1.7 nM and 6.0±3.7 nM is remarkable but consistent with data for other endogenous DAMPs, such as HMGB1 or biglycan.<sup>32,33</sup> Obviously, TLR2-TLR4 cooperation supports the recognition of these endogenous proteins and activates the MyD88 signaling pathway. MyD88 signaling finally activates NF-κB-dependent cytokines such as IL-6 or TNF. Theoretically, it could be possible that other TLRs or RAGE also contribute to histone recognition in a similar manner, which could not be detected in single knockout cells.

*Myd88*-deficient mice lack postischemic renal sterile inflammation,<sup>6–8</sup> a phenomenon that can now be explained by lack of immune recognition of histones or HMGB1,<sup>9</sup> and potentially other DAMPs that remain to be identified. Other studies have already documented that deletion of TLR2 or TLR4 is sufficient to significantly reduce postischemic kidney injury.<sup>6–8</sup> These data suggest that histone recognition is not the predominant element of intrarenal danger signaling in

the postischemic kidney. TLR2 and TLR4 are both expressed on intrarenal immune cells as well as on renal parenchymal cells.<sup>6–8,28,29</sup> Studies with TLR2/TLR4 bone marrow chimeric mice revealed that postischemic danger signaling *via* TLR2/TLR4 dominates in renal parenchymal cells.<sup>6,8</sup> The fact that histone neutralization protected distal but not proximal tubular epithelial cells in the postischemic kidney should relate to the fact that only distal tubular cells upregulate TLR2 and TLR4 in the postischemic kidney.<sup>30</sup> Furthermore, we have recently shown that postischemic cytokine induction in intrarenal dendritic cells is suppressed by the constitutively expressed single immunoglobulin IL-1-related receptor as well as the induction of IFN-related factor-4, two inhibitors of TLR signaling.<sup>34–36</sup>

This study identifies extracellular histones as mediators of postischemic and septic AKI. Histones are released from dying tubular epithelial cells and act as DAMPs, which require TLR2 and TLR4 for the induction of proinflammatory cytokines. Thus, renal cell injury triggers renal inflammation because the innate immune system translates the recognition of dead cell releases, such as histones, into inflammation *via* the same receptors that recognize bacterial factors during infection. Histone neutralization might be a novel option to suppress immunopathology after tissue damage.

**CONCISE METHODS**

**Animal Studies**

C57BL/6J mice, 6–12 weeks old, genetically deficient (>F6) in *Tlr1*,<sup>37</sup> *Tlr2*,<sup>22</sup> *Tlr4*,<sup>22</sup> *Cd14*,<sup>38</sup> *Tlr6*,<sup>37</sup> *Rage*,<sup>39</sup> *Myd88*,<sup>40</sup> or *Trif*<sup>41</sup> have been described. *Tlr2*- and *Tlr4*-deficient mice were crossed to produce *Tlr2/4* double-deficient mice. The respective genotype was assured by PCR from tail-tip DNA. Histones were injected (10 mg/kg body weight) into the left renal artery 12 hours after a single injection of LPS, 1 mg/kg (Sigma-Aldrich, Steinheim, Germany), at a total volume of 200 μl, as described elsewhere.<sup>19</sup> In one experiment, the histones were predigested with 500 nM activated protein C (Sigma-Aldrich). Both kidneys were harvested 24 hours later. Septic kidney injury was induced by injection with antihistone IgG, 20 mg/kg, or control IgG 2 hours before LPS injection (10 mg/kg intraperitoneally). Renal ischemia-reperfusion injury was induced under general anesthesia as described elsewhere.<sup>36</sup> In brief, both renal pedicles were clamped for 30 minutes with microaneurysm clamps (Medicon,



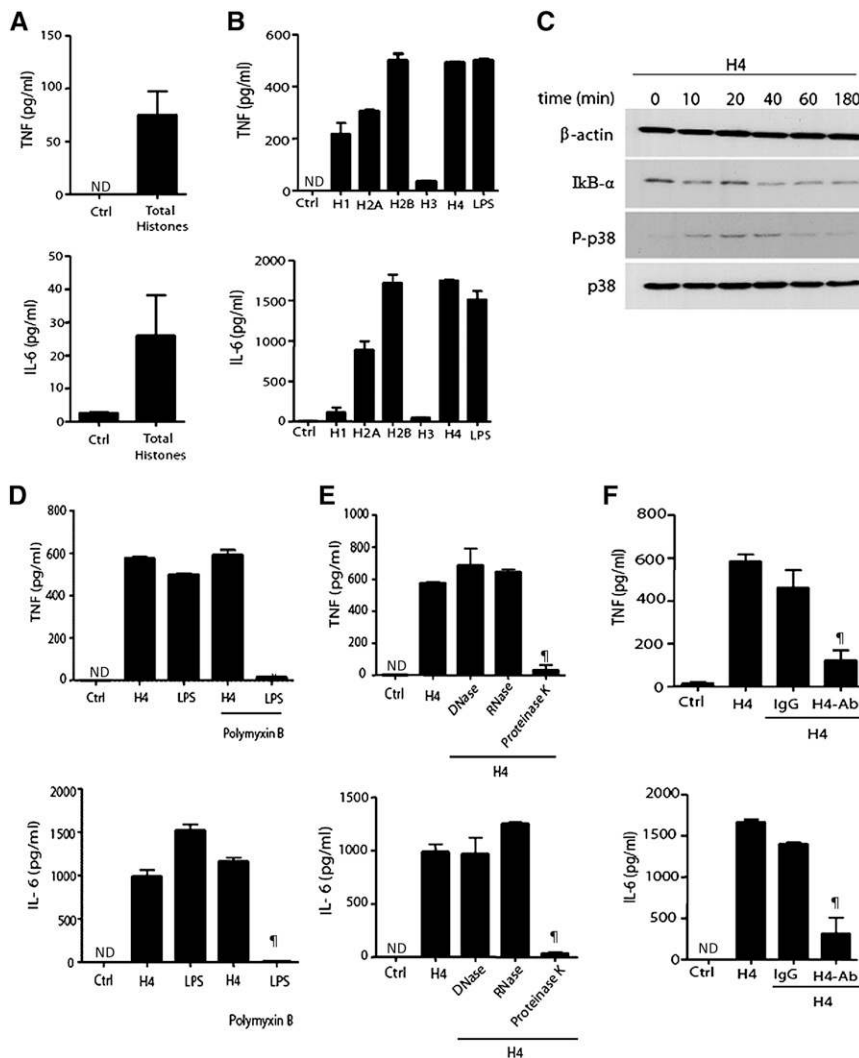


**Figure 7.** Histones activate TNF and IL-6 cytokine production. (A and B) TNF and IL-6 ELISA of supernatants from mouse BMDCs stimulated for 6 hours with total histones (30  $\mu$ g/ml) and individual histones (30  $\mu$ g/ml) or LPS (1  $\mu$ g/ml). (C) BMDCs were stimulated with H4 at the indicated time points. Cell lysates were immunoblotted and probed for the indicated proteins. (D) BMDCs were stimulated for 6 hours with H4 and LPS in the presence or absence of polymyxin B treatment. Supernatants were analyzed for TNF and IL-6 by ELISA. (E) BMDCs were stimulated for 6 hours with H4 or pretreated H4 with deoxyribonuclease, ribonuclease, and proteinase K. Supernatants were analyzed for TNF and IL-6 by ELISA. (F) BMDCs were stimulated for 6 hours with H4 in the presence or absence of anti-H4 antibodies (H4 Ab) or control IgG antibodies. Supernatants were analyzed for TNF and IL-6 by ELISA. In A, B, and D–F, the data represent the mean  $\pm$  SD of three independent experiments.  $^{\dagger}P < 0.05$  by *t* test. Data shown in part C were repeated two times. Related data are presented in Supplemental Figure 1. ND, not detected.

Tuttlingen, Germany) *via* 1-cm flank incisions. Body temperature was continuously measured with a rectal probe and maintained at 36–37°C throughout the procedure by placing the mice on a heating pad. After clamp removal, the kidney was inspected for restoration of blood flow before the wound was closed with standard sutures. Immediately after surgery or 2 hours after LPS injection, mice were intraperitoneally injected with anti-histone antibody BWA3, 20 mg/kg,<sup>18</sup> or control IgG (Abcam, Cambridge, United Kingdom). Mice

were euthanized 24 hours after reperfusion or 12 hours after LPS injection, and pieces from kidneys were harvested for further processing. All experiments were performed according to German animal protection laws and had been approved by the local government authorities.

### Assessment of Kidney Inflammation and Injury

Kidneys were embedded in paraffin, and 2- $\mu$ m sections were used for periodic acid-Schiff stains and immunostaining as described elsewhere.<sup>42</sup> Postischemic tubular injury was scored by assessing the percentage of tubules in the corticomedullary junction that displayed tubular cell flattening, cell necrosis, loss of brush border, and luminal cast formation, as follows: 0, none; 1,  $\leq 10\%$ ; 2, 11%–25%; 3, 26%–45%; 4, 46%–75%; and 5,  $>76\%$ . Septic tubular injury was scored in a same way, but ballooning and vacuolization of tubular cells were also considered as tubular damage markers.<sup>43</sup> For histochemistry we used biotinylated Lotus tetragonolobus lectin stain (Vector Labs, CA), Tamm-Horsfall protein stain (Santa Cruz Biotechnology, Inc., Santa Cruz, CA), rat antimouse neutrophils (Serotec, Oxford, United Kingdom), and the TUNEL kit (Roche, Mannheim, Germany) to quantify apoptotic cells. To count interstitial cells, 10 cortical high-power fields (400 $\times$ ) were analyzed.<sup>44</sup> BUN and creatinine were measured using urea or creatinine FS kits (DiaSys Diagnostic Systems, Holzheim, Germany) according to the manufacturer's protocols.

### In vitro Studies

Mouse renal endothelial cells were generated as recently described elsewhere.<sup>45</sup> Their proliferation was determined after 24 hours using Cell-Titer 96 Cell Proliferation Assay (Promega, Madison, WI) reading absorbance at 492 nm. BMDCs were generated by established protocols as described elsewhere.<sup>46</sup> Necrotic cell supernatants were prepared from mouse tubular cells by repeated freezing and thawing or hydrogen peroxide (H<sub>2</sub>O<sub>2</sub>; 1mM) treatment for 24 hours. RPMI 1640 GlutaMAX-I medium (Invitrogen, Carlsbad, CA) was supplemented with 10% (vol/vol) FBS (Biochrom AG, Berlin, Germany), 1% of penicillin and streptomycin (PAA Laboratories GmbH, Pasching, Austria). OptiMEM reduced-serum medium was from Invitrogen. We purchased ATP; ultrapure LPS (from *Escherichia coli* strain K12); p1:C RNA; Pam3Cys; CpG (InvivoGen, San Diego, CA); poly(dA-dT)•poly(dT-dA) sodium salt; crude LPS (*E. coli* serotype 0111:B4); N-acetyl-L-cysteine (Sigma-Aldrich, St. Louis, MO); cytochalasin D; latrunculin B (Enzo Lifesciences

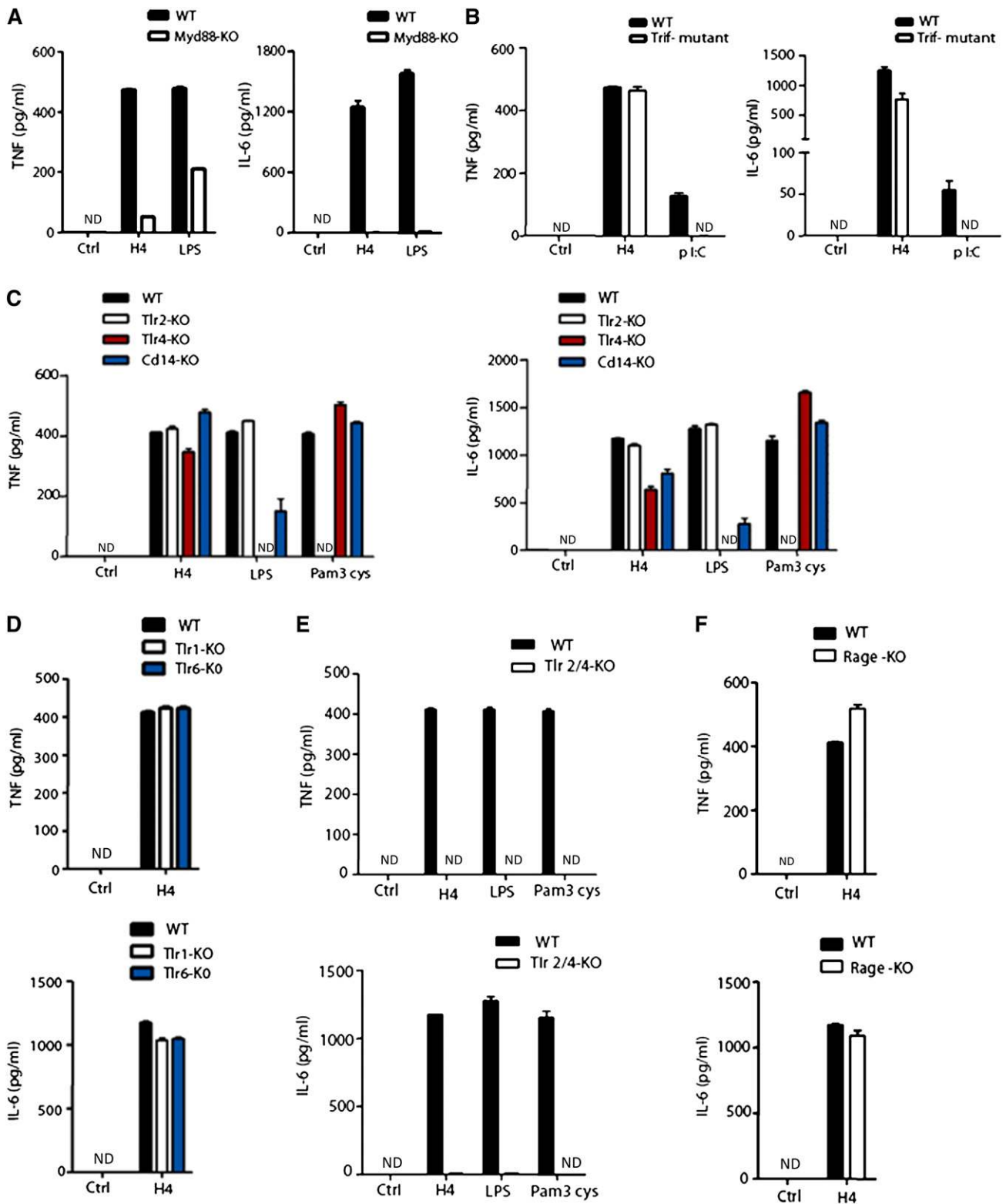


**Figure 8.** Histone H4 activates TLR2/TLR4-MyD88 to induce cytokines. ELISA for TNF and IL-6 in supernatants from wild-type (WT) and different gene-deficient BMDCs stimulated with H4 (30  $\mu$ g/ml), LPS (1  $\mu$ g/ml), Pam3Cys (1  $\mu$ g/ml), and Poly I:C RNA (5  $\mu$ g/ml) for 6 hours as indicated. A–F illustrate dendritic cell stimulation with histones and various other TLR agonists in wild-type or gene-deficient mice as indicated. The data represent the mean  $\pm$  SD of three independent experiments. #Not detected. See also Supplemental Figures 2 and 3. ND, not detected.

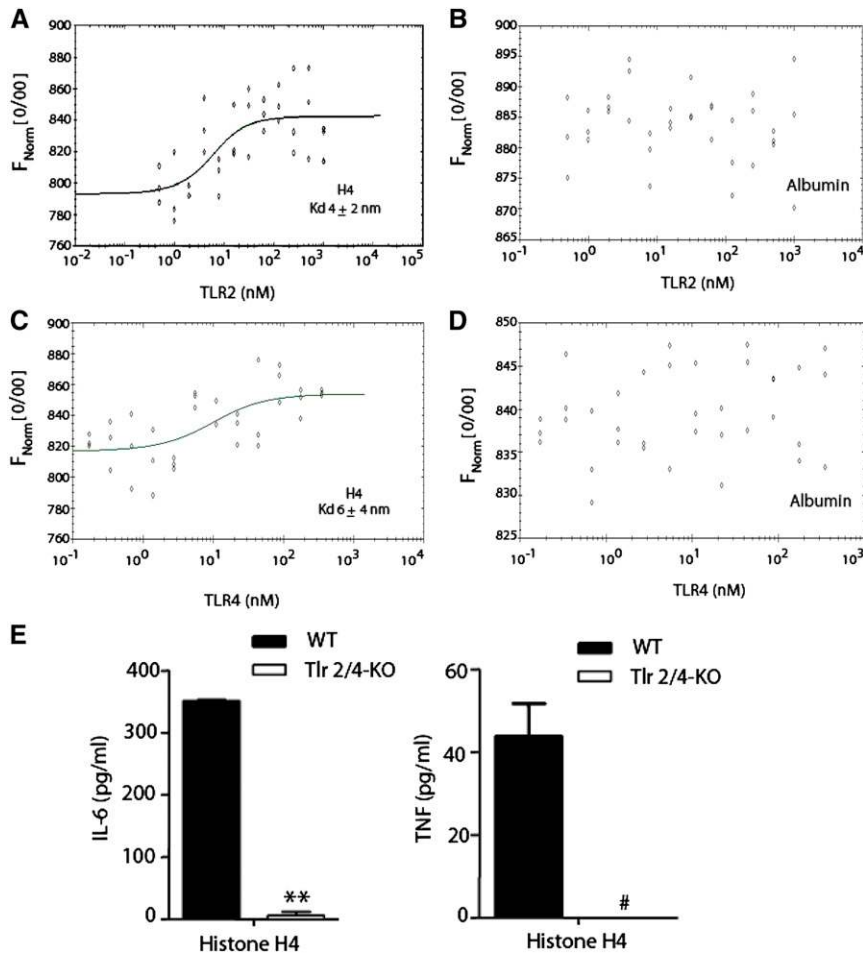


**Figure 9.** Histone H4 directly interacts with TLR2 and TLR4/MD2. (A and C) Binding of NT-647 fluorescence-labeled H4 to recombinant human TLR2 (A) and TLR4/MD2 complex (C). To determine the affinity of binding, a titration series of TLR2 (1000–1.95 nM) and TLR4/MD2 proteins (350–0.68 nM) was performed while fluorescence-labeled H4 was kept at a constant concentration of 5 nM. The change in the thermophoretic signal of H4 suggested a  $K_d$  of  $4.2 \pm 1.7$  nM for TLR2 and  $6.0 \pm 3.7$  nM for TLR4/MD2.  $K_d$  was calculated from three independent thermophoresis measurements using NanoTemper software. The fluorescence was measured before laser heating ( $F_{\text{initial}}$ ) and after 30 seconds of laser on time ( $F_{\text{hot}}$ ). The normalized fluorescence  $F_{\text{norm}} = F_{\text{hot}}/F_{\text{initial}}$  reflects the concentration ratio of labeled molecules.  $F_{\text{norm}}$  is plotted directly and multiplied by a factor of 10, yielding the relative change in fluorescence per mill ( $F_{\text{norm}} [\%]$ ). (B and D) NT-647 fluorescence-labeled albumin (5 nM) tested for its binding to TLR2 (B) and TLR4/MD2 (D) was used as negative control. (E) Mice were injected intravenously with histone H4 (20 mg/kg). After 6 hours, IL-6 and TNF cytokines were measured in plasma by ELISA. The data represent mean  $\pm$  SD from four mice in each group. \*\* $P < 0.01$  by  $t$  test. #Not detected. KO, knockout; WT, wild-type.

GmbH, Lörrach, Germany); ammonium pyrrolidine dithiocarbamate (Alexis, Lörrach, Germany); chloroquine; camptothecin (Sigma-Aldrich); CA-074-Me (Calbiochem, Darmstadt, Germany); calf thymus-derived total histones ( $^1\text{H}$  and H3; Roche Diagnostics GmbH, Mannheim, Germany); human recombinant H4, H2A, and H2B (Millipore, Billerica, MA); and control mouse IgG (Abcam PLC, Cambridge, United Kingdom). We generated mouse antibodies to H4 (BWA3) from autoimmune mice as described elsewhere.<sup>47</sup> All cells

were stimulated in serum free RPMI 1640 medium (Invitrogen) at a density of  $1 \times 10^6$  cells/ml. Cells were stimulated for 6 hours with total histones (50  $\mu\text{g/ml}$ );  $^1\text{H}$ , H2A, H2B, H3, and H4 (30  $\mu\text{g/ml}$ ); LPS (1  $\mu\text{g/ml}$ ); pI:C RNA (5  $\mu\text{g/ml}$ ); Pam3Cys (1  $\mu\text{g/ml}$ ); and poly (dA:dT) (5  $\mu\text{g/ml}$ ) transfected with Lipofectamine 2000 according to the manufacturer's protocol (Invitrogen). Latrunculin B (3  $\mu\text{M}$ ), cytochalasin D (5  $\mu\text{M}$ ), chloroquine (5  $\mu\text{g/ml}$ ), cathepsin B inhibitor CA-074-Me (10  $\mu\text{M}$ ), and N-acetyl-L-cysteine (50 mM) were added before 30 minutes of stimulation. Cell culture supernatants were analyzed for IL-6 and TNF cytokine secretion by ELISA according to the manufacturer's instructions (BD Pharmingen, San Diego, CA).

### Flow Cytometry

Flow cytometric analyses of endothelial cells were performed on an FACS Calibur flow cytometer (BD Biosciences) as described elsewhere.<sup>48</sup> Cells were stimulated with CpG, camptothecin, or histones for 3, 6, or 24 hours, respectively. Supernatants were used for analysis because dead cells dissolved from the plate membrane and moved into fluid media. Every supernatant was counted for their cell amounts, then washed with PBS and incubated with binding buffer containing FITC-anti-annexin V (BD, Franklin Lakes, NJ) or propidium iodide (BD Biosciences) for 15 minutes at room temperature.

### RNA Preparation and Real-Time RT-PCR

Reverse transcription and real-time PCR from total renal RNA was prepared as described elsewhere.<sup>36</sup> SYBR Green Dye detection system was used for quantitative real-time PCR on Light Cycler 480 (Roche, Mannheim, Germany). Gene-specific primers (300 nM; Metabion, Martinsried, Germany) were used as listed in Table 1. Controls consisting of ddH<sub>2</sub>O were negative for target and housekeeper genes.

### Western Blotting

Precipitated media supernatants or cell extracts were analyzed by standard immunoblot technique as described elsewhere.<sup>46</sup> Anti- $\text{I}\kappa\text{B-}\alpha$ , anti-phospho p38, anti-total p38, and anti-histone H4 antibodies were from Cell Signaling Technology (Danvers, MA).

### Histone 4-TLR2/TLR4 Binding Assay Using Microscale Thermophoresis

Protein-protein interactions of histone H4 with recombinant human TLR2 or human TLR4/MD2 complex (both from R&D Systems) were

**Table 1.** Primers used for real-time RT-PCR

Target	Primer Sequence
CXCL2	Forward primer 5'-CGGTCAAAAAGTTTGCCTTG-3' Reverse primer 5'-TCCAGGTCAGTTAGCCTTGC-3'
CXCL10	Forward primer 5'-ATGGATGGACAGCAGAGAGC-3' Reverse primer 5'-GGCTGGTCACCTTTCAGAAG-3'
CCL5	Forward primer 5'-GTGCCACGTCAAGGAGTAT-3' Reverse primer 5'-CCACTTCTTCTCTGGGTTGG-3'
ICAM-1	Forward primer 5'-AACAGTTCACCTGCACGGAC-3' Reverse primer 5'-GTCACCGTTGTGATCCCTG-3'
IL-6	Forward primer 5'-TGATGCACTTGCAGAAAACA-3' Reverse primer 5'-ACCAGAGGAAATTTTCAATAGGC-3'
IL12	Forward primer 5'-AGTCCCTTTGGTCCAGTGTG-3' Reverse primer 5'-AGCAGTAGCAGTCCCCTGA-3'
KIM-1	Forward primer 5'-TGGTTGCCTTCCGTGTCTCT-3' Reverse primer 5'-TCAGCTCGGGAATGCACAA-3'
Nos2	Forward primer 5'-TGAAGAAAACCCCTTGTGCT-3' Reverse primer 5'-TTCTGTGCTGTCCCAGTGAG-3'
TNF- $\alpha$	Forward primer 5'-CCACCACGCTCTTCTGTCTAC-3' Reverse primer 5'-AGGGTCTGGGCCATAGAACT-3'
18s RNA	Forward primer 5'-GCAATTATCCCCATGAACG-3' Reverse primer 5'-AGGGCCTCACTAAACCATCC-3'

ICAM, intercellular adhesion molecule.

determined by changes in the thermophoretic movement of NT-647 fluorescence-labeled (Monolith NT<sup>T</sup> Protein Labeling Kit, NanoTemper Technologies GmbH, Munich, Germany) histone H4 using the microscale thermophoresis binding assay (NanoTemper Technologies).<sup>49</sup> A titration series of TLR2 (1000–1.95 nM) and TLR4/MD2 proteins (350–0.68 nM), each diluted 1:1 with PBS containing 0.0025% Tween 20 and 0.5% BSA, was performed. The concentration of NT-647 fluorescence-labeled H4 was kept constant (5 nM). The TLRs were incubated with H4 for 30 minutes in the dark to enable binding. The reaction was then aspirated into glass capillaries and sealed with wax, and the thermophoretic movement of labeled H4 was monitored with a laser on for 30 seconds and off for 5 seconds at a laser voltage of 60%. To demonstrate that the changed thermophoresis of H4 was actually due to its interaction with TLR2 or TLR4/MD2, NT-647 fluorescence-labeled albumin (5 nM, Thermo Fisher Scientific) was tested for its binding to TLR2 and TLR4 in the same experimental setting as negative controls. Fluorescence was measured before laser heating (F initial) and after 30 seconds of laser on time (F hot). The normalized fluorescence  $F_{norm} = F_{hot}/F_{initial}$  reflected the concentration ratio of labeled molecules.  $F_{norm}$  was plotted directly and multiplied by a factor of 10, yielding a relative change in fluorescence per milliliter.  $K_d$  was calculated from three independent thermophoresis measurements using NanoTemper Software (NanoTemper Technologies).

### In Vivo Microscopy on Mouse Cremaster Muscles

The surgical procedure and the technical setup for *in vivo* microscopy and dextran permeability of the cremaster muscle have been described elsewhere.<sup>50</sup> After 6 hours of intrascrotal stimulation with histones (500  $\mu$ g), *in vivo* microscopy was performed. For the

quantitative analysis of the leukocyte migration measures, CapImage software (Dr. Zeintl, Heidelberg, Germany) was used. Firmly adherent cells were determined as those resting in the associated blood flow for more than 30 seconds and related to the luminal surface per 100- $\mu$ m vessel length. Transmigrated cells were counted in regions of interest covering 75  $\mu$ m on both sides of a vessel over 100  $\mu$ m of vessel length. For measurement of centerline blood flow velocity, green fluorescent microspheres (2- $\mu$ m diameter; Molecular Probes, Leiden, the Netherlands) were injected *via* an arterial catheter, and their passage through the vessels of interest was recorded using the FITC filter cube under appropriate stroboscopic illumination (exposure 1 millisecond, cycle time 10 millisecond,  $\lambda = 488$  nm). From measured vessel diameters and centerline blood flow velocity, apparent wall shear stress was calculated, assuming a parabolic flow velocity profile over the vessel cross section.<sup>51</sup> As a measure of microvascular permeability, five postcapillary vessel segments as well as the surrounding perivascular tissue were excited at 488 nm, and emission >515 nm was recorded by a CCD camera (Sensicam, PCO, Kelheim, Germany) 30 minutes after injection of FITC-dextran (Sigma Aldrich) using an appropriate emission filter (LP 515). Mean gray values of fluorescence intensity were measured by digital image analysis (TILLvisION 4.0, TILL Photonics) in six randomly selected regions of interest (50 $\times$ 50  $\mu$ m<sup>2</sup>), localized approximately 50  $\mu$ m distant from the venule under investigation. Phenotyping of transmigrated leukocytes was performed on paraffin-embedded tissue sections immunostained with rat-anti-mouse CD45, Ly6G, or F4/80 mAb (Serotec, Oxford, United Kingdom) and counterstained with Mayer's hemalaun.<sup>52</sup>

### Statistical Analyses

Data were expressed as mean  $\pm$  SD. Comparison between two groups was performed by two-tailed *t* test. A *P* value < 0.05 was considered to represent a statistically significant difference. All statistical analyses were calculated using Graph Pad Prism (GraphPad Software, Inc., La Jolla, CA).

### ACKNOWLEDGMENTS

We thank Shizuo Akira for Myd88 knockout mice; Bruce Butler for Trif mutant mice; M. Sperandio for RAGE knockout mice; and Jürgen Heesemann for TLR1, TLR6, and CD14 knockout mice. The expert technical assistance of Dan Draganovic, Janina Mandelbaum, Sandy Walther, and Claudia Schwarzenberg is gratefully acknowledged.

This work was supported by SFB 815, Project A5, and SCHA 1082/2-1 to L.S. This work was funded by grants from the Deutsche Forschungsgemeinschaft (GRK1202, AN372/9-2, and AN372/14-1) to H.J.A. and SFB 914 Project B3 to C.A.R. and F.K.

### DISCLOSURES

None.

## REFERENCES

- Bonventre JV, Zuk A: Ischemic acute renal failure: an inflammatory disease? *Kidney Int* 66: 480–485, 2004
- Swaminathan S, Griffin MD: First responders: understanding monocyte-lineage traffic in the acutely injured kidney. *Kidney Int* 74: 1509–1511, 2008
- Rock KL, Latz E, Ontiveros F, Kono H: The sterile inflammatory response. *Annu Rev Immunol* 28: 321–342, 2010
- Kono H, Rock KL: How dying cells alert the immune system to danger. *Nat Rev Immunol* 8: 279–289, 2008
- Lichtnekert J, Vielhauer V, Zecher D, Kulkarni OP, Clauss S, Segerer S, Hornung V, Mayadas TN, Beutler B, Akira S, Anders HJ: Trif is not required for immune complex glomerulonephritis: Dying cells activate mesangial cells via Tlr2/Myd88 rather than Tlr3/Trif. *Am J Physiol Renal Physiol* 296: F867–F874, 2009
- Leemans JC, Stokman G, Claessen N, Rouschop KM, Teske GJ, Kirschning CJ, Akira S, van der Poll T, Weening JJ, Florquin S: Renal-associated TLR2 mediates ischemia/reperfusion injury in the kidney. *J Clin Invest* 115: 2894–2903, 2005
- Shigeoka AA, Holscher TD, King AJ, Hall FW, Kiosses WB, Tobias PS, Mackman N, McKay DB: TLR2 is constitutively expressed within the kidney and participates in ischemic renal injury through both MyD88-dependent and -independent pathways. *J Immunol* 178: 6252–6258, 2007
- Wu H, Chen G, Wyburn KR, Yin J, Bertolino P, Eris JM, Alexander SI, Sharland AF, Chadban SJ: TLR4 activation mediates kidney ischemia/reperfusion injury. *J Clin Invest* 117: 2847–2859, 2007
- Wu H, Ma J, Wang P, Corpuz TM, Panchapakesan U, Wyburn KR, Chadban SJ: HMGB1 contributes to kidney ischemia reperfusion injury. *J Am Soc Nephrol* 21: 1878–1890, 2010
- Zhai Y, Shen XD, O'Connell R, Gao F, Lassman C, Busuttill RW, Cheng G, Kupiec-Weglinski JW: Cutting edge: TLR4 activation mediates liver ischemia/reperfusion inflammatory response via IFN regulatory factor 3-dependent MyD88-independent pathway. *J Immunol* 173: 7115–7119, 2004
- Oyama J, Blais C Jr, Liu X, Pu M, Kobzik L, Kelly RA, Bourcier T: Reduced myocardial ischemia-reperfusion injury in toll-like receptor 4-deficient mice. *Circulation* 109: 784–789, 2004
- Shishido T, Nozaki N, Yamaguchi S, Shibata Y, Nitobe J, Miyamoto T, Takahashi H, Arimoto T, Maeda K, Yamakawa M, Takeuchi O, Akira S, Takeishi Y, Kubota I: Toll-like receptor-2 modulates ventricular remodeling after myocardial infarction. *Circulation* 108: 2905–2910, 2003
- Tang SC, Arumugam TV, Xu X, Cheng A, Mughal MR, Jo DG, Lathia JD, Siler DA, Chigurupati S, Ouyang X, Magnus T, Camandola S, Mattson MP: Pivotal role for neuronal Toll-like receptors in ischemic brain injury and functional deficits. *Proc Natl Acad Sci U S A* 104: 13798–13803, 2007
- Anders HJ: Toll-like receptors and danger signaling in kidney injury. *J Am Soc Nephrol* 21: 1270–1274, 2010
- Kawasaki H, Iwamuro S: Potential roles of histones in host defense as antimicrobial agents. *Infect Disord Drug Targets* 8: 195–205, 2008
- Papayannopoulos V, Zychlinsky A: NETs: A new strategy for using old weapons. *Trends Immunol* 30: 513–521, 2009
- Chaput C, Zychlinsky A: Sepsis: The dark side of histones. *Nat Med* 15: 1245–1246, 2009
- Xu J, Zhang X, Pelayo R, Monestier M, Ammollo CT, Semeraro F, Taylor FB, Esmon NL, Lupu F, Esmon CT: Extracellular histones are major mediators of death in sepsis. *Nat Med* 15: 1318–1321, 2009
- Hohenstein B, Kuo MC, Addabbo F, Yasuda K, Ratliff B, Schwarzenberger C, Eckardt KU, Hugo CP, Goligorsky MS: Enhanced progenitor cell recruitment and endothelial repair after selective endothelial injury of the mouse kidney. *Am J Physiol Renal Physiol* 298: F1504–F1514, 2010
- Huang H, Evankovich J, Yan W, Nace G, Zhang L, Ross M, Liao X, Billiar T, Xu J, Esmon CT, Tsung A: Endogenous histones function as alarmins in sterile inflammatory liver injury through Toll-like receptor 9 in mice. *Hepatology* 54: 999–1008, 2011
- Kessenbrock K, Krumbholz M, Schönemarker U, Back W, Gross WL, Werb Z, Gröne HJ, Brinkmann V, Jenne DE: Netting neutrophils in autoimmune small-vessel vasculitis. *Nat Med* 15: 623–625, 2009
- Takeuchi O, Hoshino K, Kawai T, Sanjo H, Takada H, Ogawa T, Takeda K, Akira S: Differential roles of TLR2 and TLR4 in recognition of gram-negative and gram-positive bacterial cell wall components. *Immunity* 11: 443–451, 1999
- Schaefer L, Babelova A, Kiss E, Hauser HJ, Baliova M, Krzyzankova M, Marsche G, Young MF, Mihalik D, Götte M, Malle E, Schaefer RM, Gröne HJ: The matrix component biglycan is proinflammatory and signals through Toll-like receptors 4 and 2 in macrophages. *J Clin Invest* 115: 2223–2233, 2005
- Scaffidi P, Misteli T, Bianchi ME: Release of chromatin protein HMGB1 by necrotic cells triggers inflammation. *Nature* 418: 191–195, 2002
- Gowda NM, Wu X, Gowda DC: The nucleosome (histone-DNA complex) is the TLR9-specific immunostimulatory component of *Plasmodium falciparum* that activates DCs. *PLoS ONE* 6: e20398, 2011
- Xu J, Zhang X, Monestier M, Esmon NL, Esmon CT: Extracellular histones are mediators of death through TLR2 and TLR4 in mouse fatal liver injury. *J Immunol* 187: 2626–2631, 2011
- Hakkim A, Füllrohr BG, Amann K, Laube B, Abed UA, Brinkmann V, Herrmann M, Voll RE, Zychlinsky A: Impairment of neutrophil extracellular trap degradation is associated with lupus nephritis. *Proc Natl Acad Sci U S A* 107: 9813–9818, 2010
- Pawar RD, Castrezana-Lopez L, Allam R, Kulkarni OP, Segerer S, Radomska E, Meyer TN, Schwesinger CM, Akis N, Gröne HJ, Anders HJ: Bacterial lipopeptide triggers massive albuminuria in murine lupus nephritis by activating Toll-like receptor 2 at the glomerular filtration barrier. *Immunology* 128[Suppl]: e206–e221, 2009
- Tsuboi N, Yoshikai Y, Matsuo S, Kikuchi T, Iwami K, Nagai Y, Takeuchi O, Akira S, Matsuguchi T: Roles of toll-like receptors in C-C chemokine production by renal tubular epithelial cells. *J Immunol* 169: 2026–2033, 2002
- Wolfs TG, Buurman WA, van Schadewijk A, de Vries B, Daemen MA, Hiemstra PS, van 't Veer C: In vivo expression of Toll-like receptor 2 and 4 by renal epithelial cells: IFN-gamma and TNF-alpha mediated up-regulation during inflammation. *J Immunol* 168: 1286–1293, 2002
- Zarjou A, Agarwal A: Sepsis and acute kidney injury. *J Am Soc Nephrol* 22: 999–1006, 2011
- Parroche P, Lauw FN, Goutagny N, Latz E, Monks BG, Visintin A, Halmen KA, Lamphier M, Olivier M, Bartholomeu DC, Gazzinelli RT, Golenbock DT: Malaria hemozoin is immunologically inert but radically enhances innate responses by presenting malaria DNA to Toll-like receptor 9. *Proc Natl Acad Sci U S A* 104: 1919–1924, 2007
- Park JS, Svetkauskaite D, He Q, Kim JY, Strassheim D, Ishizaka A, Abraham E: Involvement of toll-like receptors 2 and 4 in cellular activation by high mobility group box 1 protein. *J Biol Chem* 279: 7370–7377, 2004
- Gong J, Wei T, Stark RW, Jamitzky F, Heckl WM, Anders HJ, Lech M, Rössle SC: Inhibition of Toll-like receptors TLR4 and 7 signaling pathways by SIGIRR: A computational approach. *J Struct Biol* 169: 323–330, 2010
- Lassen S, Lech M, Römmele C, Mittrüecker HW, Mak TW, Anders HJ: Ischemia reperfusion induces IFN regulatory factor 4 in renal dendritic cells, which suppresses postischemic inflammation and prevents acute renal failure. *J Immunol* 185: 1976–1983, 2010
- Lech M, Kulkarni OP, Pfeiffer S, Savarese E, Krug A, Garlanda C, Mantovani A, Anders HJ: Tir8/Sigirr prevents murine lupus by suppressing the immunostimulatory effects of lupus autoantigens. *J Exp Med* 205: 1879–1888, 2008
- Netea MG, van de Veerdonk F, Verschuereen I, van der Meer JW, Kullberg BJ: Role of TLR1 and TLR6 in the host defense against disseminated candidiasis. *FEMS Immunol Med Microbiol* 52: 118–123, 2008

38. Perera PY, Vogel SN, Detore GR, Haziot A, Goyert SM: CD14-dependent and CD14-independent signaling pathways in murine macrophages from normal and CD14 knockout mice stimulated with lipopolysaccharide or taxol. *J Immunol* 158: 4422–4429, 1997
39. Liliensiek B, Weigand MA, Bierhaus A, Nicklas W, Kasper M, Hofer S, Plachky J, Gröne HJ, Kurschus FC, Schmidt AM, Yan SD, Martin E, Schleicher E, Stern DM, Hämmerling G G, Nawroth PP, Arnold B: Receptor for advanced glycation end products (RAGE) regulates sepsis but not the adaptive immune response. *J Clin Invest* 113: 1641–1650, 2004
40. Kawai T, Adachi O, Ogawa T, Takeda K, Akira S: Unresponsiveness of MyD88-deficient mice to endotoxin. *Immunity* 11: 115–122, 1999
41. Hoebe K, Du X, Georgel P, Janssen E, Tabeta K, Kim SO, Goode J, Lin P, Mann N, Mudd S, Crozat K, Sovath S, Han J, Beutler B: Identification of Lps2 as a key transducer of MyD88-independent TIR signalling. *Nature* 424: 743–748, 2003
42. Kulkarni O, Pawar RD, Purschke W, Eulberg D, Selve N, Buchner K, Ninichuk V, Segerer S, Vielhauer V, Klusmann S, Anders HJ: Spiegelmer inhibition of CCL2/MCP-1 ameliorates lupus nephritis in MRL-(Fas)pr mice. *J Am Soc Nephrol* 18: 2350–2358, 2007
43. Wang Y, Huang WC, Wang CY, Tsai CC, Chen CL, Chang YT, Kai JI, Lin CF: Inhibiting glycogen synthase kinase-3 reduces endotoxaemic acute renal failure by down-regulating inflammation and renal cell apoptosis. *Br J Pharmacol* 157: 1004–1013, 2009
44. Ninichuk V, Khandoga AG, Segerer S, Loetscher P, Schlapbach A, Revesz L, Feifel R, Khandoga A, Krombach F, Nelson PJ, Schlöndorff D, Anders HJ: The role of interstitial macrophages in nephropathy of type 2 diabetic db/db mice. *Am J Pathol* 170: 1267–1276, 2007
45. Akis N, Madaio MP: Isolation, culture, and characterization of endothelial cells from mouse glomeruli. *Kidney Int* 65: 2223–2227, 2004
46. Allam R, Darisipudi MN, Rupanagudi KV, Lichtnekert J, Tschopp J, Anders HJ: Cutting edge: Cyclic polypeptide and aminoglycoside antibiotics trigger IL-1 $\beta$  secretion by activating the NLRP3 inflammasome. *J Immunol* 186: 2714–2718, 2011
47. Monestier M, Fasy TM, Losman MJ, Novick KE, Muller S: Structure and binding properties of monoclonal antibodies to core histones from autoimmune mice. *Mol Immunol* 30: 1069–1075, 1993
48. Allam R, Sayyed SG, Kulkarni OP, Lichtnekert J, Anders HJ: Mdm2 promotes systemic lupus erythematosus and lupus nephritis. *J Am Soc Nephrol* 22: 2016–2027, 2011
49. Wienken CJ, Baaske P, Rothbauer U, Braun D, Duhr S: Protein-binding assays in biological liquids using microscale thermophoresis. *Nat Commun* 1: 100, 2010
50. Khandoga AG, Khandoga A, Anders HJ, Krombach F: Postschismic vascular permeability requires both TLR-2 and TLR-4, but only TLR-2 mediates the transendothelial migration of leukocytes. *Shock* 31: 592–598, 2009
51. Hägele H, Allam R, Pawar RD, Reichel CA, Krombach F, Anders HJ: Double-stranded DNA activates glomerular endothelial cells and enhances albumin permeability via a toll-like receptor-independent cytosolic DNA recognition pathway. *Am J Pathol* 175: 1896–1904, 2009
52. Reichel CA, Khandoga A, Anders HJ, Schlöndorff D, Luckow B, Krombach F: Chemokine receptors Ccr1, Ccr2, and Ccr5 mediate neutrophil migration to postschismic tissue. *J Leukoc Biol* 79: 114–122, 2006

---

See related editorial, "Dying Cells and Extracellular Histones in AKI: Beyond a NET Effect?," on pages 1275–1277.

This article contains supplemental material online at <http://jasn.asnjournals.org/lookup/suppl/doi:10.1681/ASN.2011111077/-/DCSupplemental>.